ARTICLE

Binding of Dengue Virus Particles and Dengue Proteins onto Solid Surfaces

Edla. M. A. Pereira,[†] Aline F. Dario,[†] Rafael F. O. França,[‡] Benedito A. L. Fonseca,[§] and Denise F. S. Petri*[,†]

Instituto de Química, Universidade de São Paulo, P.O. Box 26077, 05513-970 São Paulo, Brazil, Programa de Pós Graduação em Imunologia Básica e Aplicada, Faculdade de Medicina de Ribeirão Preto, Universidade de São Paulo, Ribeirão Preto, Departamento de Clínica Médica, Faculdade de Medicina de Ribeirão Preto, Universidade de São Paulo, Ribeirão Preto

ABSTRACT The interaction between dengue virus particles (DENV), sedimentation hemagglutinin particles (SHA), dengue virus envelope protein (Eprot), and solid surfaces was investigated by means of ellipsometry and atomic force microscopy (AFM). The surfaces chosen are bare Si/SiO_2 wafers and Si/SiO_2 wafers covered with concanavalin A (ConA), jacalin (Jac), polystyrene (PS), or poly(styrene sulfonate) (PSS) films. Adsorption experiments at pH 7.2 and pH 3 onto all surfaces revealed that (i) adsorption of DENV particles took place only onto ConA under pH 7.2, because of specific recognition between glycans on DENV surface and ConA binding site; (ii) DENV particles did not attach to any of the surfaces at pH 3, suggesting the presence of positive charges on DENV surface at this pH, which repel the positively charged lectin surfaces; (iii) SHA particles are positively charged at pH 7.2 and pH 3 because they adhered to negatively charged surfaces at pH 7.2 and repelled positively charged layers at pH 3; and (iv) SHA particles carry polar groups on the surface because they attached to silanol surfaces at pH 3 and avoided hydrophobic PS films at pH 3 and pH 7.2. The adsorption behavior of Eprot at pH 7.2 revealed affinity for ConA > Jac > PSS > PS ≈ bare Si/SiO_2 layers. These findings indicate that selectivity of the Eprot adsorption is higher when it is part of virus structure than when it is free in solution. The correlation between surface energy values determined by means of contact angle measurements and DENV, SHA, or Eprot adsorption behavior was used to understand the intermolecular forces at the interfaces. A direct correlation was not found because the contributions from surface energy were probably surpassed by specific contributions.

KEYWORDS: lectin • dengue virus • ellipsometry • AFM • surface energy • polystyrene

INTRODUCTION

A large number of biotechnological devices are based on the immobilization of biomolecules onto solid surfaces. One can play with the intrinsic characteristics of each system in order to achieve adsorption of the desired biomolecule (1). For instance, in the case of charged supports, the adsorbed amount of proteins can be controlled by pH and ionic strength of the medium (2). On the other hand, the attachment of proteins onto uncharged supports is mainly governed by van der Waals interaction and H bonding, which can be tuned by the support wettability (3). The surface hydration also plays a decisive role on the preservation of the natural conformation of proteins upon adsorbing. However, extremely hydrated surfaces might be inadequate for protein adsorption. Poly(ethylene glycol) enriched surfaces tend to repel proteins due to high hydration and excluded volume (4, 5). In the case of cells (6, 7) and bacteria (8), adhesion to solid surfaces seems to be controlled by the support surface energy.

Plants lectins are glycoproteins that play a very important role in biological processes because of the specific carbohydrate recognition. For example, lectins are able to detect specific glycan portions, making them important agents in blood-group identification and also for stimulating cell-surfaces receptors (9, 10). Concanavalin A (ConA) is a legume lectin mainly obtained from Jack Bean (*Canavalia ensiformis*), which binds specifically to mannose and glucose in the presence of Mn^{2+} and Ca^{2+} (11). Jacalin (Jac) is a D-galactose-binding lectin extracted from the jackfruit seeds (*Artocarpus integriofolia*) (12, 13). Different from ConA, the hemagglutinating activity of jacalin is not influenced by bivalent cations such as Ca^{2+}, Mg^{2+}, and Mn^{2+}. Immobilized ConA (14) and Jac (15) are often used in the development of bioassays or in the separation of glycoproteins from human plasma (16). In a recent report (17), we have shown that dengue fever virus particles (DENV) can be immobilized onto polysaccharides and onto ConA films, but in the case of ConA films the attachment of viral particles can be suppressed by the addition of mannose (5 mmol/L) to the medium. These findings indicated specific recognition of virus particles by ConA molecules. One argument that supports this idea is the structure of the envelope protein (Eprot) located at the surface of dengue virus, which mediates viral attachment and entry by membrane fusion. Eprots carry glycans (18, 19), which might recognize ConA binding site. However, in the presence of mannose, ConA binding

* Corresponding author. E-mail: dfsp@iq.usp.br. Tel.: 0055 11 30913831. Fax: 0055 11 3815 5579.

Received for review May 19, 2010 and accepted August 6, 2010

[†] Instituto de Química, Universidade de São Paulo.

[‡] Programa de Pós Graduação em Imunologia Básica e Aplicada, Universidade de São Paulo.

[§] Departamento de Clínica Médica, Universidade de São Paulo.

DOI: 10.1021/am100442f

Published on Web 08/17/2010

sites would be screened by mannose molecules and Eprot could no longer recognize ConA molecules. In order to gain deeper insight about the interfacial interactions between virus and surfaces, this work investigated the adhesion of DENV and Eprot onto ConA films, Jac films, Si/SiO_2 wafers, polystyrene (PS), and poly(styrene sulfonate) (PSS) by means of ellipsometry and atomic force microscopy (AFM). The correlation between surface energy properties, determined by means of contact angle measurements, and DENV or Eprot adsorption behavior was used to understand the intermolecular forces at the interfaces.

MATERIALS

Silicon ⟨100⟩ wafers purchased from Wafers University (Massachusetts, USA) with a native oxide (SiO_2) layer approximately 2 nm thick were cut in peaces of approximately 1 cm^2 of area and rinsed as described elsewhere (20). After this they were characterized by ellipsometry. Polysytrene ($M_v \sim 90\ 000$ g/mol) was kindly provided by BASF (Ludwigshafen, Germany). H_2SO_4 (96%, Casa Americana, São Paulo, Brazil), $CaCl_2$ (Casa Americana, São Paulo, Brazil), $MnCl_2$ (Vetec Química Fina, São Paulo, Brazil) and mannose (Sigma, Brazil) were analytical grade and used without further purification.

Jacalin (Jac), from *Artocarpus integriofolia* was purchased from Sigma (L3515, St. Louis, USA). It is a two-chain lectin consisting of an α chain of 133 amino acid residues bound to a β chain of 20 or 21 amino acid residues. In the tetrameric form, it has molecular weight of ~65 000 g mol^{-1} (21) and it exhibits a number of protein bands in the isoelectric point (pI) range of 4.5−8.5 (22). Concanavalin A (ConA), type IV, from *C. ensiformes*, was purchased from Sigma (C2010,St. Louis,USA). ConA monomer presents molecular weight 25 583 g mol^{-1}, pI between 4.5 and 5.6, and requires both calcium and manganese ions at each of its four saccharide binding sites (23, 24). At neutral and alkaline pH, ConA exists as a tetramer of four identical subunits. Below pH 5.6, ConA dissociates into active dimers (25).

Dengue virus type 1 (Mochizuki strain) was grown in C6/36 cells cultured in L15 Leibowitz medium supplemented with 2% of heat-inactivated fetal bovine serum and antibiotics. Viruses were added to infect confluent cell monolayers and then incubated for 1 h at 28 °C with periodic rocking every 15 min. Infected cell culture supernatants were collected 7 days after virus infection, centrifuged to clear remaining cells and cell debris, aliquoted, and frozen at −80 °C. The virus infection was then determined by RT-PCR using primers serotype specific (26). To prepare high titers of dengue virus, we concentrated supernatants of infected cell cultures in a Millipore Centricon Centrifugal Filter Unit of a 100-kDa cutoff (Amicon; Millipore) by centrifugation.

METHODS

PS and PSS Films Preparation. PS solutions were prepared in toluene at 10 g/L and deposited onto Si/SiO_2 wafers in a Headway spin-coater at 3000 rpm, during 30 s. Part of the spin-coated PS films was sulfonated by covering PS film surface with H_2SO_4 96% during 30 s, as described elsewhere (27). The sulfonation of PS at benzene p-position leads to PSS. PS and PSS films were characterized by means of contact angle measurements, ellipsometry, and atomic force microscopy (AFM).

Production of Eprot. The premembrane (prM) and envelope (E) genes of dengue-2 virus were synthesized and cloned in vector pPICZ alpha-A (invitrogen Life Sciences, USA). The recombinant plasmid were expressed in *Pichia pastoris* X33 strain and purified by metal chelating chromatography (Ni^{2+} sepharose column). Briefly, a sequence of 2001bp corresponding to genes prM and E of dengue-2 virus was amplified using the primers 5′-CCC GAA TTC TTC CAT CTG ACC ACC CGA GGG-3′ (prM gene of dengue-2) and 5′-GGG GTA CCG GCG CCT GAA CCA TGA CTC CTA-3′ (envelope gene of dengue-2). These primers introduced an *Eco*RI and a *Kpn*I cleavage site, respectively. The target fragment was amplified of extracted RNA from dengue-2 virus by RT-PCR using the kit Qiagen One Step RT-PCR Kit, (Qiagen, USA) with the following protocol: 50 °C 30 min, 95 °C 15 min, followed by 94 °C 30 s, 55 °C 1 min, and 68 °C 2 min for 40 cycles, and finally 72 °C for 10 min. The amplified DNA fragment was digested by *Eco*RI and *Kpn*I and then ligated into the expression vector pPICZ alpha-A using T4 DNA ligase, accordingly to manufacturer's instructions, after ligation the reaction was used to transform competent bacteria (*E. coli* DH5α). The insert in the recombinant plasmid, obtained from the selected colonies cultivated in LB selective media, was confirmed by restriction endonuclease digestion with the same endonucleases and by DNA sequencing.

After confirmation of the correct plasmid construction, the recombinant linearized plasmid pPICZ alpha-A-DENV2 (cleaved with PstXI endonuclease) was transformed into competent *P. pastoris* X33 cells by electroporation. The transformants were selected on YPD medium containing 1000 μg mL^{-1} zeocin (Invitrogen Life Sciences). The positive transformants were identified by direct PCR screening of the colonies employing the primers cited above and then cultured in BMGY medium at 220 rpm at 30 °C for approximately 20 h; after this period, the cells were spinned down and the media changed by BMMY supplemented with methanol 0.5% for protein expression induction, the cells were cultivated by a total of 3 days at 220 rpm at 30 °C; after 3 days, the supernatant was collected and analyzed by SDS-PAGE and Western blot with mice antidengue antibody.

After recombinant protein detection (Eprot) by Western blot, we performed large scale expression for protein purification. Briefly, transformed yeast cells were cultivated as cited and the supernatant was collected, filtered through a 0.45 μm filter and then the applied to a Ni^{2+} saturated chelating sepharose column (GE Healthcare, USA) pre-equilibrated with binding buffer (20 mM Na_3PO_4, 0.5 M NaCl, 20 mM Imidazole, pH 7.4). The fusion recombinant protein was eluted with a gradient of 0−1 M imidazole.

Lectin Adsorption onto Si/SiO_2 Wafers. Jacalin (Jac) solution was prepared in 0.20 mol/L PBS (pH 7.2) at the concentration of 0.20 g/L. ConA was dissolved at pH 5.0 in the presence of 0.01 mol/L $MnCl_2$ and 0.01 mol/L $CaCl_2$, so that the final concentration of the lectin amounted to 0.20 mg/mL (28). Si/SiO_2 wafers were dipped into the lectin solutions for 3 h at (25 ± 1)° C. Thereafter, the wafers were removed, gently rinsed with distilled water and dried under N_2 stream and finally characterized by means of contact angle measurements, ellipsometry, and AFM.

Adsorption of Dengue Viruses. Dengue virus dispersions prepared at 4 mg/mL under pH 7.2 (0.20 mol/L PBS) or pH 3 were allowed to interact with Si/SiO_2 wafers, PS films, PSS films and lectin-covered surfaces during 3 h at (36 ± 1)°C. In another set of experiments virus dispersions were prepared at 4 mg/mL and pH 7.2 (0.20 mol/L PBS) in the presence of mannose or galactose (at final concentration 0.005 mol/L) prior to adsorption onto ConA or Jac films, respectively. After this the samples were rinsed with distilled water, dried under N_2 stream and characterized by contact angle measurements, ellipsometry, and AFM.

Adsorption of Eprot. Aqueous solution of dialyzed E protein was prepared at 10 μg/mL. Si/SiO_2 wafers, PS films, PSS films and lectin covered Si/SiO_2 wafers were immersed into Eprot solution at 36 °C during 3 h. In another set of experiments Eprot solution was prepared at 10 μg/mL in the presence of (i) mannose at 0.005, 0.050, or 0.100 mol/L prior to adsorption

onto ConA films or (ii) galactose at 0.005 mol/L prior to adsorption onto Jac films. After that, the samples were removed from the solution, rinsed with pure water, dried under a N_2 stream and characterized by contact angle measurements, ellipsometry, and AFM.

Desorption Experiment. Desorption experiments were performed by dipping the adsorbate (lectin or virus or Eprot)-covered substrates into pure solvent. After 8 h, they were removed from the solutions and dried under a stream of N_2, and the thickness was monitored by means of ellipsometry.

Contact Angle Measurements. Contact angle measurements were performed at (24 ± 1) °C in a home-built apparatus (29) using sessile drops of 8 μL. To determine the surface energy (γ_S) of PS, PSS and lectin films contact angles θ were performed with diiodomethane (>99.5%, purely dispersive nature) and distilled water (polar liquid) (29−31). To use Young's equation without correction for roughness and chemical heterogeneity (32), only very smooth and homogeneous films were used. At least three films of the same sample were analyzed. The polar (γ^p) and dispersive (γ^d) components of the surface energy were determined by Owens-Wendt's (33) equation, also known as geometric mean equation.

Ellipsometry. Ellipsometric measurements were performed in the air at (24 ± 1)° C, using a vertical computer-controlled DRE-EL02 ellipsometer (Ratzeburg, Germany). The angle of incidence was set at 70.0° and the wavelength, λ, of the He−Ne laser was 632.8 nm. For data interpretation, a multilayer model composed by the substrate, the unknown layer and the surrounding medium should be used. Then the thickness (D) and refractive index (n) of the unknown layer can be calculated from the ellipsometric angles, Δ and Ψ, using the fundamental ellipsometric eq 1 and iterative calculations with Jones matrices (34)

$$e^{i\Delta}\tan\psi = R_p/R_s = f(n, D, \lambda, \phi) \quad (1)$$

where R_p and R_s are the overall reflection coefficients for the parallel and perpendicular polarization. Measurements can be performed in situ so that Δ and Ψ are determined every 4 s. They are a function of the angle of incidence ϕ, the wavelength λ of the radiation, the refractive index n, and the thickness D of each layer of the model.

In this work, a multilayer model was composed by silicon, silicon dioxide, adsorbed layers (PS, PSS, lectins, Eprot, or virus particles), and the surrounding medium (air). First of all, the thickness of the SiO_2 layers was determined in air, considering the refractive index for Si as $n = 3.88 - i0.018$ (35) and its thickness as an infinite one, for the surrounding medium (air) the refractive index, n, was considered as 1.00. Because the native SiO_2 layer is very thin, its n was set as 1.462 (35) and the thickness value D of SiO_2 layer in each wafer was determined individually. The indices of refraction for PS and PSS amounted to 1.583 and 1.588, respectively (27). The indices of refraction for lectins and viruses were set as 1.52 (28) and 1.50, respectively, and just the layer thickness was calculated. One must be aware that ellipsometry yields the mean thickness based on a model, which considers the adsorbed layer as a homogeneous isotropic smooth layer. The mean thickness is an average over peaks and valleys in a spot area of 3 mm^2. Therefore, AFM is a perfect complement for ellipsometry because it allows visualizing the adsorbed layer topography.

Atomic Force Microscopy (AFM). Atomic force microscopy (AFM) measurements were performed in a PICO SPM-LE (Molecular Imaging) microscope in the intermittent contact in air at room temperature, using silicon cantilevers with resonance frequency close to 300kHz. Scan areas ranging from (1 μm × 1 μm) to (500 nm × 500 nm) were obtained with resolution of 512 × 512 pixels. Image processing and the determination of the root-mean-square (rms) were performed using the Pico Scan software. At least three films of the same composition were analyzed at different areas of the surface.

Table 1. Ellipsometric Layer Thickness, Mean Surface Roughness (rms) Determined by Means of AFM and Contact Angle Measurements for Each Supporting Layer

outermost layer	layer thickness (nm)	layer roughness (nm)	θ_{water} (deg)
SiO_2	1.9 ± 0.1	0.3 ± 0.1	5 ± 1
ConA	2.5 ± 0.5	0.8 ± 0.2	51 ± 3
Jac	1.8 ± 0.2	1.0 ± 0.2	48 ± 2
PS	48 ± 3	0.4 ± 0.2	90 ± 1
PSS	46 ± 2	0.5 ± 0.2	64 ± 5

RESULTS AND DISCUSSION

Support Layers. Table 1 shows the characteristics of support layers. The mean thickness of SiO_2 onto bare wafers was (1.9 ± 0.1) nm. They are very smooth (rms 0.3 ± 0.1 nm) and hydrophilic. A typical AFM image obtained for clean Si/SiO_2 wafers is provided as the Supporting Information (Figure SI 1a). The adsorption of ConA onto Si/SiO_2 wafers from solutions at pH 5.0, which favors tetrameric arrangement, led to films (2.5 ± 0.5) nm thick. The adsorption of ConA molecules onto Si/SiO_2 wafers is probably driven by electrostatic interaction between ConA positively charged residues and deprotonated silanol groups on the surface (28). The adsorption of Jac molecules onto Si/SiO_2 wafers took place at pH 7.2, where they exist predominantly as tetramers. Considering that Jac has pI in the pH range of 7−8.5 (13), the adsorption onto Si/SiO_2 wafers also might be favored by electrostatic interactions between positively charged Jac residues and negatively charged Si/SiO_2 wafers surfaces. Jac films mean thickness amounted to (1.8 ± 0.2) nm. Desorption experiments were performed after adsorption of ConA or Jac onto Si/SiO_2 wafers by exchanging lectin solution by pure buffer and monitoring the mean D values of adsorbed particles by ellipsometry. The changes in D values were on the order of ±5%, indicating irreversible adsorption of lectins onto Si/SiO_2 wafers. Both ConA and Jac molecules formed densely packed layers on the surface (AFM images provided as Supporting Information, Figures SI 1b,c), yielding similar mean roughness values. As expected, the highest wettability was observed for bare Si/SiO_2 wafers (5 ± 1)°, whereas contact angles measured for ConA and Jac were (51 ± 3)° and (48 ± 2)°, respectively, indicating the exposition of polar residues to the air. The mean thickness values obtained for PS and PSS amounted to (48 ± 3) nm and (46 ± 2) nm, respectively. They are thicker than the lectin films because they were spin-coated from concentrated solution (10 g/L). After sulfonation, the contact angle of water onto PS films decreased from (90 ± 1)° to (64 ± 5)°. In a previous work (27), we have shown by fluorescence microscopy that PSS films are not homogeneously sulfonated, but there are sulfonated patches on the surface that increase the wettability. PS films are very smooth (rms = 0.4 ± 0.1 nm), but became slightly rougher after sulfonation

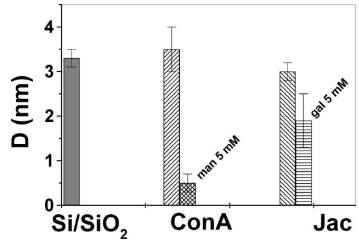

FIGURE 1. Mean ellipsometric thickness (*D*) values determined for dengue virus particles onto bare Si/SiO_2 wafers, ConA (in the absence and in the presence of mannose 5 mmol/L), and Jac layers (in the absence and presence of galactose 5 mmol/L).

reaction (rms = 0.5 ± 0.1 nm). AFM images obtained for PS and PSS films are shown as Supporting Information (Figures SI 1d,e).

Adsorption of Dengue Virus Particles onto Solid Support. Mature infectious dengue viruses (DENV) are icosahedral, ~50 nm in diameter (comprising an electron dense core of 30 nm and a lipid envelope) and present smooth surface (36). Dengue virus dispersions used for the adsorption experiments contain DENV, particles secreted by dengue virus and remainder proteins from culture medium. Sedimentation hemagglutinins (SHA) are particles secreted by dengue virus and present typical diameter of 14 nm (18, 36).

Figure 1 shows that the mean ellipsometric thickness (D) values determined for virus particles adsorbed from pH 7.2 onto bare Si/SiO_2 wafers, ConA and Jac covered Si/SiO_2 wafers were similar (~3.4 ± 0.2) nm. Therefore, the mean *D* values indicate that neither bare Si/SiO_2 wafers nor lectins surfaces were fully covered by dengue particles. On the other hand, no adsorption was observed for dengue particles onto PS or PSS films. The hydrophobicity of PS surface and the random distribution of sulfonate groups onto PSS (27) probably made these substrates unattractive for virus particle immobilization.

Considering the silica pI of 2.8 (37) and Jac and Con A pIs ranging from 4.5 to 8.5 (22) and from 4.5 to 5.6 (23, 24), respectively, at pH 7.2 bare Si/SiO_2 wafers, ConA and Jac layers are negatively charged. The adsorption of virus particles (DENV and SHA) onto bare Si/SiO_2 wafers, ConA and Jac layers might be driven by electrostatic interaction. To reduce the charge density onto Si/SiO_2 wafers and to enrich ConA and Jac layers with positive charges due to aminoacid protonation, we also performed adsorption experiments at pH 3. The mean thickness values (*D*) found for adsorbed virus particles at pH 3 was (3.6 ± 0.3) nm, which is similar to the *D* values determined at pH 7.2 (3.2 ± 0.2 nm). Therefore, in the case of bare Si/SiO_2 wafers, the adsorption of virus particles is equally favored when the surface is enriched by negative charges (SiO^-) or by hydroxyl groups (SiOH). On the contrary, the acidic condition disfavored the adsorption of virus particles onto positively charged ConA and Jac layers or onto polymeric films; at pH 3, *D* values ranged from null to (0.20 ± 0.05 nm).

After virus particle adsorption onto ConA and Jac layer the mean surface roughness values increased from (0.8 ± 0.1 nm) to (1.6 ± 0.2 nm) and from (1.0 ± 0.2 nm) to (1.4 ± 0.2 nm), respectively.

Ellipsometry and model calculations yield a mean thickness value under the assumption that the layer is isotropic and homogeneous. Comparing *D* values in the range of 3.0−3.5 nm (Figure 1) with typical sizes of DENV (30 nm) and SHA (10−15 nm), one cannot distinguish which sort of particle has adsorbed; one can conclude only that the surface is not fully covered by particles. That is why AFM is an excellent complementary technique for ellipsometry. AFM topographic images allow revealing the morphology and homogeneity of surfaces. Tools available in the AFM software allow calculating the mean roughness values and the height of isolated particles. One should notice that the isolated particle height is reliable information, while the particle width carries tip convolution effects, which enlarge the lateral size (38). If the size and form of the tip are well-known, convolution effects can be corrected to estimate particles width (28, 38). In the present work, particle height was analyzed and particle width calculation was avoided because tip characteristics were not precise.

AFM images (Figure 2) were obtained for particles adsorbed at pH 7.2. They show that particles are sparsely distributed on the surfaces, corroborating with *D* values. When bare Si/SO_2 wafers were used as supports (Figure 2a), a compact layer formed by small entities densely packed, which might be correlated with cell culture medium proteins, and some few higher structures. Some of these high structures are aggregates and some of them are isolated particles with height ~14 nm (Figure 2b). We analyzed 30 other isolated particles (not shown) distributed on the same sample and on replicates, which in a similar way were not perfectly spherical and presented height ranging from 10 to 18 nm. Considering these dimensions, these particles might be attributed to SHA particles. Aggregated and isolated particles were observed onto ConA surfaces (Figure 2c,d). Part of the isolated particles presented height ranging from 25 to 30 nm (Figure 2e), which might be correlated with the dengue particle (DENV) core, because the lipid envelope probably has collapsed upon drying; and the other one varying from 10 to 15 nm (Figure 2f), which might be attribute to adsorbed SHA particles. Such profiles were found for replicates, totaling 30 different scan regions, and the bimodal size distribution was reproducible. Aggregates and isolated particles smaller than ~15 nm were observed onto Jac layers, as evidenced in images g and h in Figure 2. The particles ~10−15 nm high might be attributed to SHA particles.

The heights estimated from topographic images indicate that the mean thickness (D) determined by ellipsometry (Figure 1) corresponded to scarcely adsorbed DENV particles and SHA particles when ConA was the surface, but when bare Si/SiO_2 wafers or Jac layers were used as supports only some SHA particles adsorbed. DENV particles recognized only mannose/glucose binding sites, as those present in ConA structure, but did not recognize either galactose binding sites, as those in Jac structure, or hydrophilic silanol

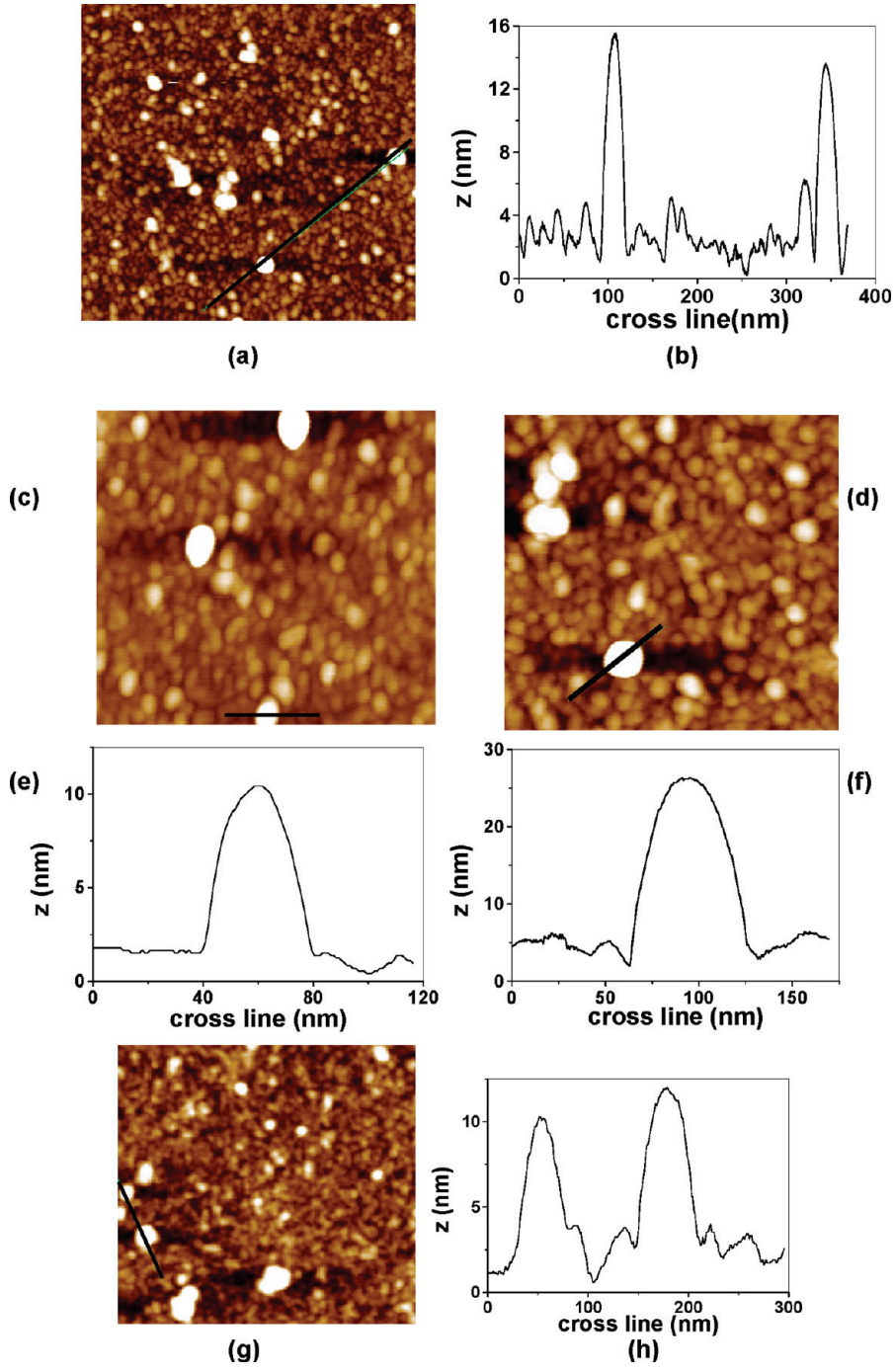

FIGURE 2. AFM topographic images obtained for adsorbed particles onto (a) bare Si/SiO_2 wafers (500 nm ×500 nm), $Z = 10$ nm, with (b) corresponding cross-section; (c, d) ConA layers (different samples) (500 nm × 500 nm), $Z = 20$ nm for both, with (e, f) corresponding cross-sections obtained for isolated particles; (g) Jac layer (750 nm ×750 nm), $Z = 10$ nm and (h) corresponding cross-section.

groups onto Si/SiO_2 wafers. To verify if this conclusion is correct, we added mannose or galactose (at final concentration 0.005 mol/L) to virus dispersion prior to adsorption onto ConA or Jac films, respectively. When mannose was added to the system, the adsorption of DENV particles was suppressed because D values decreased from (3.5 ± 0.3) nm to (0.5 ± 0.2) nm (Figure 1). In the presence of mannose, the presence of particles ~25 and ~15 nm high are less frequent, as presented in Figure 3a. These findings shows that mannose reduced virus particles adhesion in ~86% and supports the conclusion that the attachment of dengue virus particles onto lectins is probably driven by recognition of mannose binding site as depicted in Figure 4a. Nevertheless, when ConA binding sites are occupied by mannose, virus particles could no longer recognize specific bindings sites on the surface, and then adsorption does not take place (Figure 4b). Such binding site blocking was also revealed by the substantial reduction in the mean adhesion force between carboxymethylcellulose decorated particles and ConA monolayers when mannose was added to the system (39). In the case of Jac surfaces, when galactose was added to the system, the mean thickness of adsorbed virus (D) decreased

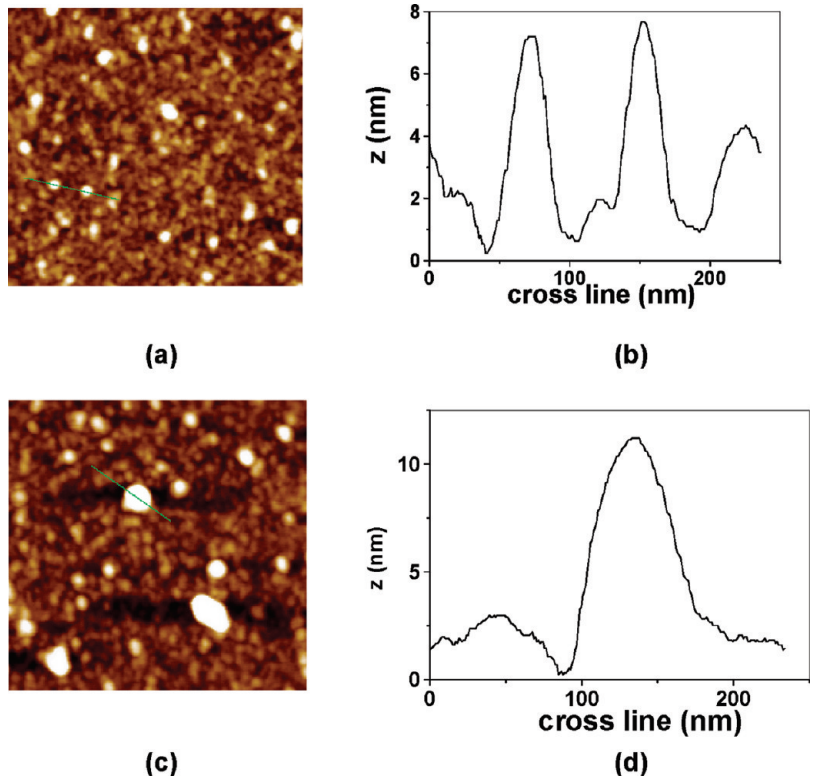

FIGURE 3. AFM topographic images obtained for adsorbed particles onto (a) ConA layer in the presence of mannose 0.005 mol/L (720 nm × 720 nm), $Z = 10$ nm, with (b) corresponding cross-sections obtained for isolated particles; (c) Jac layer in the presence of galactose 0.005 mol/L (750 nm × 750 nm), $Z = 10$ nm and (d) corresponding cross-section.

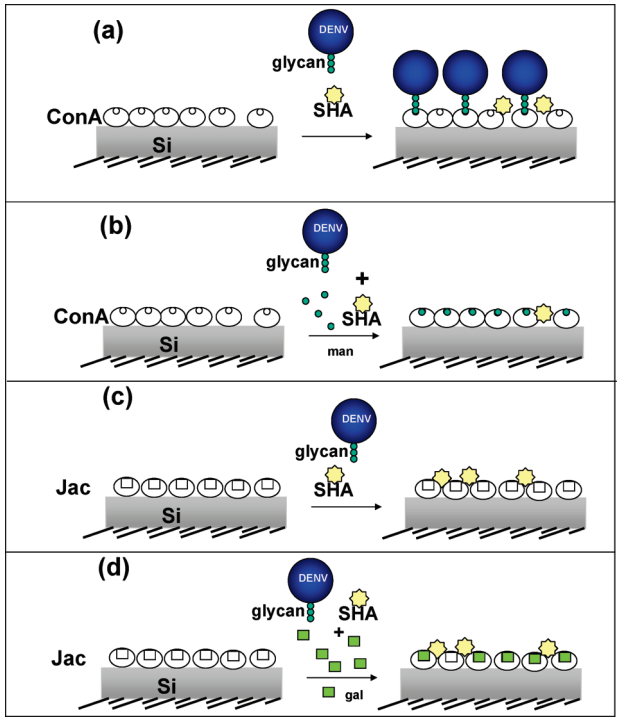

FIGURE 4. Schematic representation of (a) specific interaction between ConA covered Si/SiO_2 wafers and E protein glycan portion and unspecific binding of DHS onto ConA layers; (b) suppression of DENV adsorption due to the presence of mannose (circles); (c) unspecific interaction between Jac covered Si/SiO_2 wafers and SHA secreted of dengue viruses; (d) unspecific SHA adsorption onto Jac layer in the presence of galactose (squares).

from (3.0 ± 0.6) nm to (1.9 ± 0.2) nm (Figure 1). The low reduction of ~37% in D values, indicates that the presence of galactose inhibited partially the attachment of SHA particles to Jac surface. The morphological features observed in a typical AFM topographic image obtained after adsorption of viral particles onto Jac layers in the presence of galactose (Figure 3b) are very similar to those observed in the absence of galactose (Figure 2g). Considering the high adsorption constant between jacalin and galactose (2×10^7 L/mol) (40), these findings indicate that virus particles binding to Jac surfaces are not mediated by Jac-galactose binding site, but by unspecific interactions, as depicted in schemes c and d in Figure 4.

Coming back to the ellipsometric thickness determined for adsorbed particles onto bare Si/SiO_2 wafers at pH 3, the AFM images and height values obtained for these samples were similar to those observed for adsorbed particles at pH 7.2. They indicated the presence of SHA particles and absence of DENV particles (see Figure SI 2 in the Supporting Information).

So far, results can be summarized as follows. Adsorption of DENV particles took place only onto ConA under pH 7.2 because of specific recognition between glycans on DENV surface and ConA binding site. The presence of positive charges on DENV particles surfaces at pH 3 was evidenced because they did not attach to any of the surfaces at this pH. The adsorption behavior of SHA particles at pH 7.2 and pH 3 onto all surfaces tested revealed that they carry (i) positive charges at both pHs because they adhered to negatively surfaces (at pH 7.2) and repelled positively charged layers (at pH 3) and (ii) polar groups because they attached to

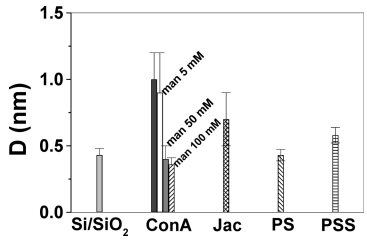

FIGURE 5. Mean ellipsometric thickness (D) values determined for Eprot onto bare Si/SiO_2 wafers, ConA layers (in the absence and in the presence of mannose 5, 50, and 100 mmol/L), Jac layers (in the absence and in the presence of galactose 5 mmol/L), PS, and PSS films.

silanol surfaces (at pH 3) and avoided hydrophobic PS films (at pH 3 and 7.2).

Desorption experiments were performed after adsorption of dengue particles onto bare Si/SiO_2, ConA or Jac layers by exchanging virus dispersion by pure solvent and monitoring the mean D values of adsorbed particles by ellipsometry. The changes in D values was on the order of $\pm 10\%$, indicating weak desorption of viral particles to lectin surfaces.

Adsorption of Eprot onto Solid Support. The infection mechanism by DENV is well-described in the literature (18). DENV are icosahedral, enveloped virus containing a single strand of a positive-sense RNA genome about 11 000 nucleotides in length. The genome codes for a long polyprotein, which comprises the structural proteins Cpror (capsid), Mprot (membrane), and Eprot (envelop) and replication proteins. The Cprot packages the viral genome and forms the nucleocapsid core, which is surrounded by a lipid membrane. Mprot and Eprot are embedded in this membrane. Therefore, in the initial stages of infection process Eprot plays a very important role, because it contains a cellular-receptor binding site. After binding to the host cell membrane, the low pH in the endosome causes conformational changes in the Eprot structure, which allow the complete fusion of the viral and host cell membranes. The nucleocapsid core is released into the cytoplasma where viral genome is uncoated. Then viral protein translation and genome replication start in the cytoplasma (41). Eprot ectodomain (residues 1−395) is composed of domains I, II, and III (18, 42, 43). Domain I, the central one, contains the N-terminus of the protein; domain II, the extended one, contains a small hydrophobic sequence that initiates the fusion process (41, 44); and domain III is supposed to be in the receptor binding. There are two potential N-linked carbohydrate sites at N67 and N-153 (42), which are glycosylated.

Considering the importance of Eprot in the infection initial stages, the adsorption of Eprot onto bare Si/SiO_2 wafers, ConA, Jac, PS, and PSS surfaces was also investigated. Contrary to virus particles, Eprot adsorbed onto all surfaces. The mean thickness values are shown in Figure 5. The highest D values were found for Eprot adsorbed onto ConA (1.0 ± 0.2) nm and Jac (0.7 ± 0.2) nm, whereas D values for Eprot onto bare Si/SiO_2 wafers, PS, and PSS films amounted to values close to (0.50 ± 0.05) nm. The addition of mannose to the Eprot solution prior to the adsorption onto

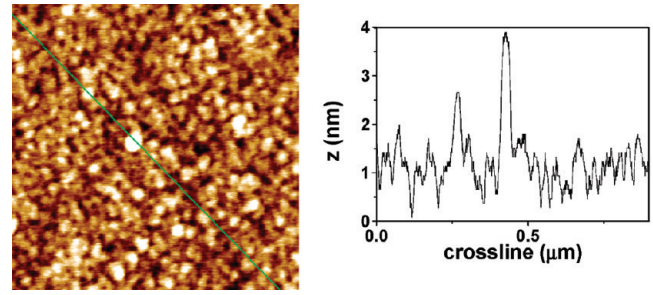

FIGURE 6. Typical AFM image ($1\ \mu m \times 1\ \mu m$) obtained for Eprot adsorbed onto PSS film with the corresponding cross-section; $Z = 7$ nm, rms = 0.5 nm.

Table 2. Contact Angle Measurements Performed with Sessile Drops of Water (θ_{water}) and CH_2I_2 ($\theta_{CH_2I_2}$) onto Surfaces for the Calculations of Dispersive (γ^d) and Polar (γ^p) Values of Surface Energy Components[a]

surface	θ°_{water} (deg)	$\theta_{CH_2I_2}$ (deg)	γ^d (mJ/m^2)	γ^p (mJ/m^2)	γ_S (mJ/m^2)
SiO_2	[b]	[b]	39	41.8	80.8
SiO_2/ConA	51 ± 3	32 ± 2	43 ± 4	16 ± 2	59 ± 6
SiO_2/Jac	48 ± 2	37 ± 4	35 ± 3	21 ± 2	56 ± 5
SiO_2/PS	90 ± 1	25 ± 3	43 ± 3	4 ± 1	47 ± 4
SiO_2/PSS	64 ± 5	30 ± 2	45 ± 1	13 ± 1	58 ± 2

[a] The total surface energy (γ_S) is given by the sum of γ^d and γ^p. [b] See ref 46.

ConA layers reduced the binding only when mannose concentration was higher than 50 mmol/L. These findings revealed that free Eprot molecules present higher affinity for ConA layers, in agreement with the results shown in Figure 1, but also that when Eprot is free in the solution and not bound to the virus surface, the degree of freedom is high and binding to a surface might occur because of hydrophobic interaction, electrostatic interaction, or H bonding. On the other hand, when Eprot is part of the virus surface, it probably has a special conformation so that adsorption becomes more selective, similarly to the conformational changes that Eprot undergoes to promote fusion (38, 41). AFM images revealed that regardless the support used for the adsorption Eprot appeared as well-packed small spherical entities on the surface (Figure 6). The addition of galactose at 0.005 mol/L had no significant effect on the D values of adsorbed Eprot onto Jac layer, indicating unspecific binding.

Support Surface Energy and Dengue Particles or Eprot Adsorption Behavior. The correlation between support surface energy and dengue particles or Eprot adsorption behavior was used to understand the intermolecular forces at the interfaces. Table 2 shows the surface energy values determined from contact angle measurements for each support. The dispersive component (γ^d) values varied from 35 to 45 mJ/m^2. This range is often found for macromolecules (6). The polar component (γ^p) was the smallest (4 mJ/m^2) for the hydrophobic PS surfaces and the largest (41.8 mJ/m^2) for the hydrophilic Si/SiO_2 wafers. Although PSS and ConA present different chemical structures, they presented similar values of γ^d and γ^p.

The adsorption of DENV or SHA particles onto PS or PSS films was not observed. Therefore, the surface energy parameters determined for the supports could not be correlated with the viral particles attachment, because although ConA and PSS presented similar surface energy components, DENV adsorbed onto ConA but not onto PSS. Curiously, the surface energy of substrate plays a very important role on cell adhesion. Cell spreading depends on the polar component of surface energy; spreading is favored when $\gamma^p > 15$ mJ/m^2 (45). The results presented here show clearly that the adhesion of virus particles (DENV and SHA) could not be ruled out by surface energy, probably because specific contributions surpassed the energetic contribution. On the other hand, the adsorption of Eprot took place regardless the substrate surface energy, evidencing that when Eprot is free in solution and not as a part of virus surface, the degree of freedom is high and binding to a surface might occur due to hydrophobic interaction, electrostatic interaction or H bonding. For instance, EProt adhered similarly to PS, which is a very hydrophobic surface ($\theta = 90° \pm 1°$), and to bare Si/SiO_2 wafer, which is a very hydrophilic ($\theta = 5° \pm 1°$) (29) surface.

The lack of adhesion of DENV to PS and PSS surfaces indicate that when Eprot is part of virus structure, Eprot hydrophobic residues are not exposed to the medium. The adsorption of DENV onto ConA surfaces indicates Eprot mannose binding sites exposition and recognition, probably the glycosylated sites at N-67 and N-153 (42).

CONCLUSIONS

The present study provided experimental evidence to support that at pH 7.2 the immobilization of DENV particles took place only onto ConA layers, as a result from specific recognition of E protein glycosylated residues and ConA mannose binding site. E protein adhesion is more selective when it is part of virus structure than when it is free in solution. The conformation of Eprot bound to DENV surface seems to expose mainly glycosylated residues to the medium. This finding can be applied for the development and design of new devices for dengue detection. Moreover, the role played by mannose during the initial stages of infection process might be explored as a strategy for infection inhibition. At pH 3, the net charge at the DENV and SHA surfaces seems to be positive; this information might be important for the development of separation/purification protocols.

Regarding the supports investigated, the role played by surface energy components on the adsorption behavior of virus particles or Eprot seems to be surpassed by specific contributions. Although surface energy is a determinant parameter for cell adhesion, in the case of virus particles, the surface energy of substrates does not necessarily dominate the adsorption process. Virus surfaces are more complex than cells and their binding seems to be particularly dependent on specific recognition.

Acknowledgment. The authors acknowledge Conselho Nacional de Desenvolvimento Científico e Tecnológico (CNPq/MCT) and Fundação de Amparo à Pesquisa do Estado de São Paulo (FAPESP) for financial support.

Supporting Information Available: Additional figures (PDF). This material is available free of charge via the Internet at http://pubs.acs.org.

REFERENCES AND NOTES

(1) Nel, A. E.; Mädler, L.; Velego, D.; Xia, T.; Hoek, E. M.; Somasundaran, P.; Klaessig, F.; Castranova, V.; Thompson, M. *Nat. Mater.* **2009**, *8*, 543.
(2) Dobrynin, A. V.; Rubenstein, M. *Prog. Polym. Sci.* **2005**, *30*, 1049.
(3) Pamu, J. E.; De; Cupere, V. M.; Rouxhet, P. G.; Dupont-Gillain, Ch. C. *J. Colloid Interface Sci.* **2004**, *278*, 63.
(4) Efremova, N. V.; Bondurant, B.; O'Brien, D. F.; Leckband, D. E. *Biochemistry* **2000**, *39*, 3441.
(5) Dobrovolskaia, M. A.; Mcneil, S. E. *Nat. Nanotechnol.* **2007**, *2*, 469.
(6) Harnett, E. M.; Alderman, J.; Wood, T. *Colloids Surf., B* **2007**, *55*, 90.
(7) Casarano, R.; Bentini, R.; Bueno, V. B.; Iacovella, T.; Monteiro, F. B. F.; Iha, F. A. S.; Campa, A.; Petri, D. F. S.; Jaffe, M.; Catalani, L. H. *Polymer* **2009**, *50*, 6218.
(8) Briandet, R.; Herry, J.-M.; Bellon-Fontaine, M.-N. *Colloids Surf., B* **2001**, *21*, 299.
(9) Taylor, E.; Drickamer, K. *Introduction to Glycobiology*, 2nd ed.; Oxford University Press, New York, 2006.
(10) Jelinek, R.; Kolusheva, S. *Chem. Rev.* **2004**, *104*, 5987.
(11) Brewer, C.; Brown, R.; Koenig, S. *Biochem.* **1983**, *22*, 3691.
(12) Bunn-Moreno, M. M.; Campos-Neto, A. *J. Immunol.* **1981**, *127*, 427.
(13) Kabir, S. *Int. J. Biochem. Cell Biol.* **1995**, *27*, 147.
(14) Turkova, J. *J. Chromatogr., B* **1999**, *722*, 11.
(15) Smith, E. A.; Thomas, W. D.; Kiessling, L. L.; Corn, R. M. *J. Am. Chem. Soc.* **2003**, *125*, 6140.
(16) Kullolli, M.; Hancock, W. S.; Hincapie, M. *J. Sep. Sci.* **2008**, *31*, 2733.
(17) Pereira, E. M. A.; Sierakowski, M. R.; Jó, T. A.; Moreira, R. A.; Monteiro-Moreira, A. C.; França, R. F. O.; Fonseca, B. A. L.; Petri, D. F. S. *Colloid Surf., B* **2008**, *66*, 45.
(18) Bock, G.; Goode, J. *New Treatment Strategies for Dengue and other Flaviviral Diseases*; Novartis Foundation Symposia Series; John Wiley & Sons: Chichester, U.K., 2006.
(19) Modis, Y.; Ogata, S.; Clements, D.; Harrison, S. C. *Proc. Natl. Acad. Sci. U.S.A.* **2003**, *100*, 6986.
(20) Fujimoto, J.; Petri, D. F. S. *Langmuir* **2001**, *17*, 56.
(21) Ruffet, E.; Paquet, N.; Frutiger, S.; Hughes, G. J.; Jaton, J. C. *Biochem. J.* **1992**, *286*, 131.
(22) Reeke, G. N.; Becker, J. W.; Edelman, G. M. *J. Biol. Chem.* **1975**, *250*, 1525.
(23) Ahmed, H.; Chatterjee, B. P. *J. Biol. Chem.* **1989**, *264*, 9365.
(24) Zand, R.; Agrawal, B.; Goldstein, I. J. *Proc. Natl. Acad. Sci. U.S.A.* **1971**, *68*, 2173.
(25) http://www.expasy.org, ID: P02866, accessed in October 2009.
(26) de Paula, S. O.; Pires Neto, R. J.; Corrêa, J. A. C. T.; Assumpção, S. R.; Costa, M. L. S.; Lima, D. M.; Fonseca, B. A. L. *Trans. R. Soc. Trop. Med. Hyg.* **2002**, *96*, 266.
(27) Petri, D. F. S.; Wenz, G.; Schunk, P.; Schimmel, T.; Dichtl, M.; Bruns, M. *Colloid Polym. Sci.* **1999**, *277*, 673.
(28) Castro, L. B. R.; Petri, D. F. S. *J. Nanosci. Nanotechnol.* **2005**, *5*, 2063.
(29) Adamson, W. A. *Physical Chemistry of Surfaces*, fifth ed.; Wiley: Toronto, 1990.
(30) Chaudhury, M. K. *Mater. Sci Eng., R* **1996**, *16*, 97.
(31) Kosaka, P. M.; Amin, J., Jr.; Saito, R. S. N.; Petri, D. F. S. Thermodynamics of Cellulose Ester Surfaces. In *Model Cellulosic Surfaces*; ACS Symposium Series; American Chemical Society: Washington, D.C., 2009; Vol. 1019, pp 223−241.
(32) Marmur, A. *Soft Matter* **2006**, *2*, 12.
(33) Owens, D. K.; Wendt, R. C. *J. Appl. Polym. Sci.* **1996**, *13*, 1741.
(34) Azzam, R. M. A.; Bashara, N. M. *Ellipsometry and Polarized Light*: North Holland, Amsterdam, 1987.
(35) Palik, E. D. *Handbook of Optical Constants of Solids*; Academic Press: London, 1985.
(36) Zhang, Y.; Corver, J.; Chipman, P. R.; Zhang, W.; Pletnev, S. W.; Sedlak, D.; Baker, T. S.; Strauss, J. H.; Kuhn, R. J.; Rossmann, M. G. *EMBO J.* **2003**, *22*, 2604.

(37) Healy, T. W.; White, L. R. *Adv. Colloid Interface Sci.* **1978**, *9*, 303.
(38) Butt, H. J.; Gerharz, B. *Langmuir* **1995**, *11*, 4735.
(39) Castro, L. B. R.; Kappl, M.; Petri, D. F. S. *Langmuir* **2006**, *22*, 3757.
(40) Smith, E. A.; Thomas, W. D.; Kiessling, L. L.; Corn, R. M. *J. Am. Chem. Soc.* **2003**, *125*, 6140.
(41) http://www.teachersdomain.org/asset/den08_vid_dengue; accessed in April 2010.
(42) Zhang, Y.; Zhang, W.; Ogata, S.; Clements, D.; Strauss, J. H.; Baker, T. S.; Kuhn, R. J.; Rossmann, M. G. *Structure* **2004**, *12*, 1607.
(43) Modis, Y.; Ogata, S.; Clements, D.; Harrison, S. C. *Nature* **2004**, *427*, 313.
(44) Allison, S. L.; Schalich, J.; Stiasny, K.; Mandl, C. W.; Heinz, F. X. *J. Virol.* **2001**, *75*, 4268.
(45) van der Valk, P.; van Pelt, A. W.; Busscher, H. J.; de Jong, H. P.; Wildevuur, C. R.; Arends, J. *J. Biomed. Mater. Res.* **1983**, *17*, 807.
(46) Cacace, M. G.; Landau, E. M.; Ramdsen, J. J. *Q. Rev. Biophys.* **1997**, *30*, 241.

AM100442F